Optimising 3D scaffold for otic neural progenitor differentiation

Kamolchanok Ngamkham[1,2], Marcelo N. Rivolta[2], Giuseppe Battaglia[1]

[1] Department of Chemistry, University College London, London, WC1H 0AJ, UK.

[2] Department of Biomedical Sciences, University of Sheffield, Sheffield, South Yorkshire, S10 2TN, UK.

_____

Correspondence to: Giuseppe Battaglia. Department of Chemistry, University College London, London, WC1H 0AJ, UK. Telephone: +44(0)2076794688; email: g.battaglia@ucl.ac.uk.

1 ABSTRACT

2   Hearing loss is a condition highly prevalent worldwide. It affects people

3 of a broad age range since the causes and risk factors are varied. At present,

4 some types of hearing impairments have a palliative treatment whereas some,

5 especially for those where otic neurons are damaged, cannot be properly

6 treated. Recent findings had shown it possible to use human embryonic stem

7 cell-derived otic neural progenitors (ONPs) as a new mode of treating hearing

8 loss caused by damage to the spiral ganglion neurons (SGNs). To improve

9 the efficiency and overcome some limitations of this potential treatment, we

10 have applied principles of tissue engineering which involves an interaction

11 between cells and an extracellular matrix –mimicking scaffold. Here, we

12 describe the influence of poly(l-lactic acid)(PLLA) aligned fibres on ONP cell

13 morphology, proliferation, neuronal differentiation and establishment of neural

14 polarity under both progenitor and neuralising conditions. The results show

15 that most of ONPs on aligned fibres exhibited bipolar morphology and

16 extended their neurites along the major fibre axis. Their proliferation was

17 lower than those in 2D culture but the differentiation of ONPs on aligned fibres

18 was significantly enhanced in both progenitor and neuralising conditions as

19 indicated by the fluorescence intensity and number of cells that were positive

20 for neuronal markers (β-tubulin III and NF200) and the expression pattern of

21 spiral ganglion molecular markers (MMP13, NPR2 and NTNG1). Moreover,

22 axonal and dendritic markers (TAU and MAP2 respectively) were also

23 induced after 14 days in culture.

24

27

28   **INTRODUCTION**

29   Hearing loss is one of the most common causes of disability. According

30   to the available data from the World Health Organization (WHO), around 360

31   million people worldwide are suffering from moderate or greater hearing loss.

32   Several types of hearing loss can be categorised according to the area of the

33   ear where the problem lies. Sensorineural hearing loss, which is caused by

34   the damage to the hair cells or the auditory nerve in the inner ear is the most

35   common. Unlike other nonmammalian vertebrates, damage or degeneration

36   of human hair cells and spiral ganglion neurons (SGNs) is irreversible [1,2].

37   Even though cochlear implants can be used to overcome a hair cell deficit,

38   loss of SGNs can limit the effectiveness of this treatment [3]. Thus, alternative

39   strategies for SGN regeneration have been widely researched and stem cell

40   therapy has been proposed as a potential therapeutic path.

41   Findings from a recent study highlight the possibility of SGNs

42   restoration using a stem cell-based strategy. Otic neural progenitors (ONPs)

43   that were differentiated from human embryonic stem cells were found to

44   exhibit true otic characteristics as indicated by the expression of several otic

45   markers such as PAX8, PAX2, SOX2 and FOXG1. They were also able to

46   further differentiate into SGNs under 'neuralising' condition, becoming positive

47   for neuronal markers, displaying appropriated membrane currents and firing

48   action potentials. When transplanted into gerbils that were deafened by the

49   application of ouabain (a model of auditory neuropathy), they engrafted and

50   significantly improved the auditory thresholds [4].

51   However, there are some potential limitations in this study that might

52   constrain a wider application of this approach. The deafness-inducing drug

53   ouabain damages primarily the type I SGNs, while type II SGNs and glial cells

54   remain mostly intact [5]. These preserved tracks might act as a guidance cue

55   for the transplanted cells, facilitating them to reach their targets centrally and

56   on the periphery. In cases were these tracts are absent, such as in a cochlear

57   nerve aplasia, ONPs might not be able to extend their neurites effectively and

58   functional restoration might be impaired. Moreover, there are some putative

59   drawbacks in delivering cells directly by cell injection. Based on evidence from

60   other experimental systems, the retention of cells at the target site and cell

61   survival rate can be poor [6,7]. To overcome those limitations, the use of a

62   support or tissue engineered scaffold mimicking the extracellular matrix may

63   be advantageous.

64   The complexity of the cochlea and sound sensing mechanism make

65   tissue engineering for the inner ear a difficult task [8]. Most of the promising

66   previous work relies on the improvement of the cochlear implant biological

67   interface. . Various reports indicated that alteration of electrode surface

68   topography, chemistry or biological functionalisation offer a great opportunity

69   for the improvement of this prostheses [9–20].

4

70   The physiological extracellular matrix of the inner ear has also been studied

71   as a natural, tissue engineered scaffold. Mice, rat and human cochlea were

72   decellularised and extracellular matrix contents, identified. However, these

73   decellularised matrices will not be appropriated for clinical application of

74   transplanted cells, and have not been widely used to support stem cell

75   differentiation [21].In this study, we aimed to investigate the behaviour of ONPs

76   on a biomaterial and explore if this scaffold could provide advantages for

77   ONP transplantation. Poly(l-lactic acid)(PLLA), a biodegradable and

78   biocompatible polymer, was fabricated as aligned electrospun fibres and used

79   as a scaffold for ONP culture. To address the effect of aligned fibres on

80   ONPs, cell attachment, proliferation, differentiation and establishment of

81   neural polarity were then analysed.

82

MATERIALS AND METHODS

Human embryonic stem cell (hESC) culture

85   Shef1 hESC line was cultured and used for the derivation of otic neural

86   progenitor. hESC colonies were maintained on inactivated mouse embryonic

87   fibroblast (MEF) feeder layers on gelatin-coated tissue culture flasks. The

88   culture media consisted of knockout Dulbecco's modified Eagle's medium

89   (Invitrogen), 20% knockout serum replacement (KOSR), 1% nonessential

90   amino acids, 2mM L-glutamine, (all from Invitrogen), 0.1mM ß-

91   mercaptoethanol (Sigma), and 4ng/ml of basic fibroblast growth factor

5

92   (bFGF; R&D systems). The colonies were passaged in clumps every 7 days

93   using collagenase and mechanical dissociating methods.

94   ***Differentiation of hES cells into otic neural progenitors (ONPs) and***

95   ***sensory neurons***

96   Generation of otic neuroprogenitors was performed as described in

97   Chen et al 2012. Briefly, undifferentiated hESCs were dissociated to single

98   cells using 0.025% trypsin-EDTA (Sigma). After trypsinization, cell suspension

99   was pelleted at 157 rcf for 5 min and passed through a 100 μm cell strainer

100   (BD Labware) to get completely dissociated cells or very small aggregates.

101   Cells were counted and plated onto laminin-coated T12.5 flasks (R&D

102   systems, 5μg/cm^2) at the seeding density of 4000 cells/cm^2. Cells were

103   maintained in a 1:1 mixture of Dulbecco's modified Eagle's medium (DMEM)

104   and F12 nutrient supplemented with N2 and B27 (DFNB). FGF3 (50ng/ml)

105   and FGF10 (50ng/ml) were added to the medium as supplements to drive the

106   differentiation [4,22]. The differentiated medium was replaced every 2 days. After

107   3-4 days, other epithelial-like and surrounding cells were scraped off to enrich

108   for ONPs. The flask was cleaned from time to time and ONPs were then

109   allowed to grow for further 10-12 days. The purified ONPs were then

110   maintained in otic stem cell full medium or OSCFM (DFNB supplemented with

111   bFGF (20ng/ml), IGF1 (50ng/ml) and EGF (20ng/ml)) and expanded on 0.1%

112   gelatin-coated flask until sufficient cell numbers were obtained.

113   Neuralisation of ONPs into auditory neurons was induced with Shh-

114   C24II (500ng/ml) , bFGF (20 ngml) and neurotrophins (NT3 and BDNF; 10

6

115 ng/ml each) added at different time points as previously described by Chen et

116 al. 2009 and 2012 [4,22].

Preparation of polylactic acid electrospun scaffolds

118 Ten percent wt. of poly(L-lactide) (PLLA) were prepared by dissolving

119 in 3:1 chloroform: methanol respectively. The solution was stirred for 1 hour at

120 room temperature or until the polymer was totally dissolved. Three ml of

121 polymer solution was electrospun from a 3 ml plastic syringe that attached to

122 a flat tip needle at constant flow rate, which was controlled by a multispeed

123 syringe pump. A high voltage (~10-12kv) was applied to the needle tip to

124 charge the polymer solution and form a liquid jet. An aluminum-rotating disk

125 was used as a grounded collector to collect the electrospun fibres. Random

126 and high alignment of fibres was collected at the rotation speed of 180 and

127 2000 rpm respectively.

Scanning electron microscopy (SEM)

129 The morphology and alignment of fibres and cells on the scaffolds were

130 visualised by SEM (Philips XL-20) at an accelerating voltage of 20 kV. Each

131 scaffold was coated with gold using a sputter coater (Emscope SC 500) prior

132 to the observation. The images were then analysed using image J software

133 (NIH).

ONP cell culture on the scaffolds

7

135   The hES-derived ONP cells were seeded onto electrospun scaffolds

136   that were sterilized in cold 70% ethanol for 15 min, washed 3 times with cold

137   PBS and incubated in OSCFM medium overnight. About 8000 ONPs were

138   seeded onto a 1 cm^2 scaffold membrane, using a very small volume (20 µl).

139   To allow attachment to the scaffold, cells were allowed to settle for one hour

140   before the medium was topped up. ONPs were then maintained in either

141   progenitor (OSCFM) or neuralising conditions for up to 14 days. Size of

142   scaffolds and cell density were scaled up for qRT-PCR gene expression

143   analysis (5×10^5 cells/ 4 cm^2 scaffold) in order to obtain good RNA yields.

144   ***SEM sample preparation for ONPs on 3D scaffolds***

145   As ONPs are loosely attached cells and most of them were not preserved

146   under normal preparation, a new preparation protocol was established

147   especially for ONPs. Culture medium was removed from the wells and the

148   cells were fixed with warm Karnovsky's fixative, which is a mixture of 2%

149   paraformaldehyde, 2.5% glutaraldehyde and 0.1M Sodium Phosphate buffer,

150   for 3 hours. ONPs were then dehydrated sequentially in 10%, 30% and 50%

151   methanol for 5 min each, followed by an air dried for 3 days. The samples

152   were dried again in a vacuum oven at room temperature overnight.

153   **Actin Staining**

154   After the cells were fixed in 4% paraformaldehyde in PBS for 1 hr, they were

155   rinsed with PBS and permeabilised with 0.3% Triton X-100 (PBST) for 15 min.

156   Three hundred and fifty µl of Texas-red-X phalloidin (1:150, Invitrogen) was

157   then added to each well and left on the rocking plate for 1 hr. The cells were

158   then rinsed with PBS after phalloidin was removed and cell nuclei were

159   counterstained with DAPI (1:200; BioLegend)

160   ***Quantification of cell directionality***

161   Fluorescent images from actin staining were used for the quantification of cell

162   directionality. The images in red channel were converted to binary images

163   using the thresholding method and the orientation of cells on binary images

164   were then analysed by orientationJ distribution, an imageJ's plugin for

165   directional analysis. The distribution of orientation histogram was

166   automatically generated from each image.

167   ***Calcein-AM staining***

168   Calcein-AM powder (Santa Cruz) was resuspended with anhydrous DMSO to

169   make a 2mM stock solution. Working solution was prepared immediately prior

170   to use by mixing Calcein-AM stock solution with the culture medium in 1:2000

171   dilutions. After the media was discarded, Calcein-AM working solution was

172   added to each well and incubated under 5% CO_2 at 37°C for 45 min. The cells

173   were then washed with media and visualised under the fluorescent

174   microscope. Intracellular esterases in live cells hydrolyse a non-fluorescent

175   Calcein-AM to strongly fluorescent Calcein, which appeared green in cell

176   cytoplasm. Numbers of Calcein positive cells from at least 10 different fields

177   were used to calculate the estimated cell number on a 1cm^2 scaffold.

178   ***BrdU Viability assay***

9

179   DNA synthesis monitoring immunofluorescence assay, 5-Bromo-2′ -

180   deoxy-uridine (BrdU) labeling and detection kit I (Roche) was used to verify

181   the viability and proliferative capacity of ONPs on the scaffolds. Ten μM BrdU

182   was added to the culture medium and incubated for 48 hr before they were

183   fixed with ethanol fixative, labelled with mouse anti-BrdU and anti-mouse

184   fluorescein. The concentration of reagents and antibodies were used

185   according to the manufacturer's instructions. Viable cells were then quantified

186   under fluorescent microscope.

187   ***Immunolabelling and quantitation of fluorescence intensity***

188   After 14 days on the scaffolds, the ONPs were fixed with 4%

189   paraformaldehyde in PBS for 1 hr and permeabilised in 0.1%Triton X-100 for

190   15 min. Then, they were incubated for 1 hr at room temperature in blocking

191   solution (0.1%Triton X-100, 5% normal donkey serum, 1% BSA in PBS)

192   before the primary antibodies were added. Double staining of β-tubulin III

193   (TUJ1) (1:100, mouse monoclonal, Covance) and NF200 (1:100, rabbit

194   polyclonal, Sigma), as well as Tau (1:50, rabbit polyclonal, Santa Cruz) and

195   MAP2 (1:200, mouse polyclonal, Abcam) were performed in this study. After

196   the cells were incubated with primary antibodies overnight at 4°C, the

197   antibodies were rinsed off and secondary donkey anti-mouse or anti-rabbit

198   antibodies conjugated with Alexa Fluor 488 or Alexa Fluor 568 (1:250,

199   Invitrogen) were applied and incubated for 1 hr at room temperature. For

200   nuclei labeling, the cells were counterstained with DAPI (1:200, 4',6-

201   diamidino-2-phenylindole; BioLegend).

202   Fluorescence intensity per cell was evaluated using ImageJ software

203   (NIH). All images were converted to black and white colour to avoid the bias.

204   Freehand selection was used to draw the area over each cells and the level of

205   fluorescence in a given region was measure as a mean grey value. This

206   number was then subtracted by the average background intensity of that

207   image.

208   ***RNA extraction and gene expression analysis***

209   Total RNA was extracted using Trizol (Invitrogen) and Qiagen RNeasy

210   column combination protocol [23]. 1 ml of Trizol was added to two 4 cm^2

211   scaffolds and pipetted up and down to dissolve the fibres. After 5 min at room

212   temperature, 200 μl of chloroform was added and mixed thoroughly. Each

213   tube was incubated for 2 min at room temperature, then spin down at 12,000

214   g for 15 min at 4°C. After the centrifugation, the transparent upper phase was

215   gently removed and transferred to a new tube. RNase-free 70% ethanol (500

216   μl) was then added and mixed well using the pipette. The mixture was

217   transferred to the RNeasy mini spin column and preceded according the

218   manufacturer protocols.

219   QuantiTect Reverse Transcription Kit (Qiagen) was used to transcribe the

220   extracted RNA to cDNA. Then, to check the expression of neural markers,

221   real-time PCR was performed using Rotor-Gene SYBR Green (Qiagen).

222   Primer sequences of housekeeping and target genes (from 5' to 3') were as

223   follows: GAPDH,   ATGGGGAAGGTGAAGGTCG   and

224   TAAAAGCAGCCCTGGTGACC; NTNG1, TTGTGGATTGGAAAGGCTGC and

225 GGTTGGAAGGGATTCAGGGA; NPR2, AACGCCATGCACCAGAAATT and

226 CATCTTCAGGCCAACAACCC; MMP13, TTGAGCTGGACTCATTGTCG and

227 TCTCGGAGCCTCTCAGTCAT.

228 *Statistical analysis*

229 All experiments were analysed using analysis of variance (one-way ANOVA)

230 followed by Bonferroni's post hoc comparison tests. Statistically significant

231 differences will be considered if the *p*-value is less than 0.05 ($p<0.05$). All

232 values are shown as mean ± standard deviation from at least 2 independent

233 experiments. All the graphs and statistic calculations were performed on

234 GraphPad Prism 6 (GraphPad Software, Inc., San Diego, CA, USA).

235

236 **RESULTS**

237 **Visualization and quantification of fibrous scaffolds**

238 After the fibres were fabricated, three independent electrospun scaffolds were

239 visualized and quantified. SEM micrograph and histogram of angle difference

240 demonstrated that most the fibres were aligned, with an average diameter of

241 0.93±0.1 µm (Figure. 1A and B). Random fibres were also fabricated and

242 characterised to be used as a control in the experiments (Figure 1C). They

243 were spun with the same set up as in aligned-fibres but the collector was

244 rotated at the lowest speed. The distributions were almost equal in all angles

245 for random fibres (Figure 1D).

12

246 **The effect of aligned PLLA fibres on ONPs morphology**

247 The morphologies of hESC-derived ONPs grown under progenitor conditions

248 (OSCFM) for 3, 7 and 14 days on aligned PLLA fibres were investigated by

249 actin staining (Texas-red Phalloidin). Nuclei were counterstained with DAPI.

250 When cultured on tissue culture plastic for a few passages, ONPs were flat

251 and spread with an average size of 300 µm (Figure 2A). On the contrary, a

252 distinct morphology was observed on 3D fibres, with cells being smaller with

253 an average size of 200 µm. After 3 days in culture, some of the ONPs were

254 spreading on the fibres (arrowhead) and elongated cells were noticed (arrow)

255 (Figure 2B). As for day 7 and 14, most of ONPs exhibited bipolar morphology

256 (69±4%) and displayed a parallel, aligned pattern in some areas of the

257 scaffold (arrow) (Figure 2C). However, cells with polygonal morphology were

258 also presented (arrowhead). In some other areas on the scaffolds,

259 randomness of ONP cell arrangement still existed (Figure 2D). On the other

260 hand, ONP growing on the random PLLA fibres were spreading in all

261 directions and showed irregular morphology (Figure 2E).

262 SEM is another method that was used to confirm the findings from fluorescent

263 imaging. ONPs indeed extend along the fibre axes and the cells with different

264 orientation or irregular shape arise from the crossing fibres presence in the

265 scaffolds (Figure 2F,G). The micrographs also revealed that single ONP cells

266 attached to few fibres at a time.

267 Orientations of cell distributions were quantified using OrientationJ plugin from

268 ImageJ. The orientation of each pixel is evaluated and plotted as a histogram

269 against the orientations in degree. The histograms demonstrated that ONPs

13

270   on 2D tissue culture plastic (Figure 2H) and PLLA random fibres (Figure 2J)

271   have broad distributions of orientation and several peaks were presented in

272   the histograms. While the cells on PLLA aligned fibres (Figure 2I) exhibited

273   one big peak, which indicated that most of the cells were arranged in a certain

274   degree.

275   **The effect of aligned PLLA fibres on ONPs viability and proliferation**

276   To check the number of viable ONP cells on the scaffolds, Calcein-AM

277   staining was carried out. After 14 days of culture, the number of viable cells

278   on neuralising 2D, control (OSCFM) PLLA and neuralising PLLA were all

279   significantly lower than those found on control (OSCFM) 2D (Figure 3A). The

280   lower numbers found on PLLA could be partially explained by the lower cell

281   attachment expected on PLLA fibres, as no bioactive sites are presented and

282   they were not treated with any chemicals or biological compounds that would

283   enhance cell attachment.. A decreased cell number under neuralising

284   condition could also infers that ONPs are differentiating into non-proliferating

285   neurons [24]. Therefore, the population of cells with dividing capability is lower.

286   It is noted that the differences between control and neuralising conditions on

287   2D were larger than those on PLLA.

288   The proliferation of ONPs was also investigated using a BrdU incorporation

289   assay (figure 3B). A significant reduction of cell proliferation, triggered by

290   culturing cells on PLLA was noticed after 3 days, regardless of the culture

291   conditions. The trend was maintained after 14 days, although the differences

292   were not large enough to remain significant. . The reduction of the percentage

293   of BrdU positive cells in neuralising conditions was, however, more obvious.

14

294   **The effect of aligned PLLA fibres on ONPs differentiation**

295   We investigated the differentiation behaviour of ONPs on PLLA electrospun

296   fibres in both conditions (progenitor and neuralising) using immunostaining of

297   the early neuronal marker β-tubulin III (TUJ1), and the mature neural marker

298   neurofilament-200 (NF200). After 14 days in culture, the expressions of TUJ1

299   and NF200 were enhanced when the cells were grown in the neuralising

300   condition or on aligned fibres (noted that cell number per area on the fibres

301   are lower than those on 2D) (Figure 4A). Mean Fluorescent intensity per cell

302   and number of positive cells for both markers were increased even without

303   any neurotrophins supplement (Figure 4B). On 2D, the intensities of both

304   markers were relatively the same in control and neuralising conditions but

305   numbers of positive cells were higher in the neuralising one. Similar trend was

306   observed on random fibres with a slight increase of fluorescence intensity.

307   The significant difference was detected only on TUJ1 between control 2D and

308   neuralising random fibres.

309   Expression of both neuronal markers studied was enhanced on ONPs seeded

310   on aligned fibres under both culture conditions. There was a clear, statistically

311   significant shift of labelling intensities (p<0.0001). This indicated that the

312   alignment of fibres alone could effectively drive the differentiation of ONPs.

313   Neuralising condition increased the neuronal marker expression on aligned

314   fibres even further and the intensity of both TUJ1 and NF200 were

315   significantly increased comparing to control condition. .

316   Several molecular markers known to be highly expressed in differentiated

317   ONPs were also explored. Matrix metalloproteinase (MMP13), natriuretic

15

318   peptide receptor2 (NPR2) and Netrin-G1 (NTNG1) [4], were used as

319   differentiation marker genes and analysed by qRT-PCR (Figure 4C). These

320   genes are upregulated in a specific manner during SGN development.

321   MMP13, also known as collagenase-3, is a zinc-dependent proteolytic

322   enzyme involved in the remodeling of ECM and is enriched at late

323   developmental stage of SGN (Lu et al., 2011; NCBI, 2016a). *NPR2* encodes

324   an integral membrane receptor for natriuretic peptides, which is required for

325   axon bifurcation in SGN and auditory circuit assembly [25,27,28]. NPR2 is highly

326   expressed at very early stage, then dropped in the middle and finally raised

327   again in the late developmental stage of SGN. *NTNG1* encodes a

328   preproprotein that can be further processed into a secreted protein, which is

329   responsible for axon growth and guidance. It is highly expressed throughout

330   the SGN development but the level is slightly higher in the early stage [25,29].

331   All three genes were upregulated when ONPs were cultured in neuralising

332   medium and on the aligned scaffolds. The increment ranged from 1 to 6 folds.

333   The upreguration of MMP13 and NPR2 on aligned fibres were even higher

334   than those on 2D neuralising conditions. On the contrary, the induction of

335   NTNG1 was maximised on 2D neuralising condition. However, due to wide

336   deviations, none of them are considered as significantly different. From the

337   pattern of gene expression that were observed, it can be inferred that after 14

338   days of differentiation, ONPs on aligned fibres are in a late developmental

339   stage.

The effect of aligned PLLA fibres on ONPs polarization

340   **The effect of aligned PLLA fibres on ONPs polarization**

341   To verify the polarisation of differentiated cells, ONPs were fixed and co-

342   stained with anti-TAU (axonal marker) and anti-MAP2 (dendritic marker)

343   antibodies after 14 days under different culture conditions. On TC plastic,

344   ONPs under progenitor condition rarely expressed TAU and MAP2 but a slight

345   increase of TAU expression was observed and cells with positive MAP2 were

346   identified under neuralising condition (Figure. 5A). On align fibres, ONPs in

347   both progenitor and neuralising conditions were positive for both neuronal

348   polarity markers. Some ONPs also showed specific localization of MAP2 in

349   the soma and TAU in both soma and axon indicating a polarization of those

350   cells (arrow). However, the majority of the cell population did not yet specify

351   their neuronal polarity. The number of positive cells was then quantified and

352   the results revealed that neuralising 2D, control PLLA and neuralising PLLA

353   can increase the percentage of TAU and MAP2 positive cells by 2 to 8 folds

354   when comparing to Control 2D group (Figure 5B). The percentages of those 3

355   conditions were comparable but the most prominent one was observed on

356   neuralising PLLA.

Discussion

357   **Discussion**

358   Not only limited to mature cells, the correlation between substrate properties

359   or microenvironment and stem cell fate has been widely investigated. Stem

360   cell differentiation is one of the main interests in tissue engineering and

361   regeneration, as in many cases the desired cell type is required prior to

362   transplantation for the safety and efficiency of the treatment [30]. It is

363   increasingly clear that the native microenvironment that supports stem cells or

17

364   'stem cell niche' plays a crucial role in the control of stem cell behaviour and

365   fate decision [31][32]. Thus, a considerable amount of work is currently being

366   performed employing this view that allows taking control over stem cells and

367   directing them to the desired behaviour.

368   Numerous studies have explored the use of electrospun fibres as tissue

369   engineering scaffolds for the repair of both central and peripheral nervous

370   system injuries [33,34]. Aligned electrospun fibres have also been used by many

371   research groups. Its advantages in neurite guiding and extension has been

372   reported *in vitro* [35–37] and the success repair were also demonstrated *in vivo*

373   [38,39]. However, those studies were performed with the cells that are not

374   directly relevant to the auditory system and tissue engineering for SGN

375   damage or degeneration has never been tried. Here, we investigated the

376   response of ONPs, a promising cell type that could be used for SGN

377   regeneration, to the aligned fibrous tissue-engineered substrate (PLLA).

378   There are many parameters that affect electrospinning process and fibre

379   morphology. They are needed to be optimised in order to achieve the ideal

380   scaffolds for each work [40]. So, in order to obtain an aligned fibre mesh with

381   the diameter of ~1 µm, which is expected to be the compromise fibre size for

382   neuronal guidance, proliferation and differentiation [41,42], electrospinning

383   parameters were manipulated. The most suitable parameters obtained were

384   used to produce aligned and random electrospun fibres. The visualisation and

385   quantification of SEM images showed that we can successfully obtain both

386   fibre types.

18

387   One of the very first ONP features that we monitored when grown on PLLA

388   fibres was cell morphology. The dissimilarity of ONPs morphology on 2D and

389   3D matrices are to be expected as the cells that were cultured on 2D tissue

390   culture plastic are flat and can only spread in horizontal plane, while on 3D,

391   which is considered to be closer to physiological conditions, cells can spread

392   in all directions [43]. The parallel cell pattern is a promising result indicating that

393   alignment of the fibres can act as a guidance cues for ONPs. Calcein-AM

394   staining and BrdU assay also demonstrated that the numbers of viable,

395   attached cells and the percentage of cell proliferation were lower on the fibres

396   comparing to 2D culture plastic. These findings are coherent with the idea

397   cells are differentiating, reducing or stopping proliferation altogether [24].

398   In previous studies of the role of scaffolds on neural differentiation,

399   experiments have been performed under neural-inducing conditions such the

400   presence of neurotrophins. However, the effect of the external scaffold on the

401   progenitors is rarely described [44–46]. From the expression of neuronal markers

402   in protein and RNA level, we clearly showed that ONPs were sensitive to the

403   change of physical environment (aligned fibres) and were able to differentiate

404   even in the normal expansion medium. Under neuralising condition, ONP

405   differentiation was increased even further. This indicated that there is a

406   synergistic effect between physical (fibre alignment) and chemical cues

407   (neuralising agents).

408   In order for neural cells to function after they are differentiated, polarization

409   and/or establishment of axons and dendrites are required [47]. Beside from

410   intrinsic factors, extracellular signal also controls polarity specification as the

19

411   neural cells are physiologically surrounded by extracellular matrix. Various

412   axonal guidance and repellent molecules have been identified to effectively

413   control the asymmetric growth of neurites and leads to axon or dendrite

414   formation [48,49]. Some growth factors such as NT3 and BDNF that were used in

415   our differentiation medium also help enhancing neuronal polarization [50,51]. As

416   we previously found that ONPs are differentiated on the aligned fibres and lots

417   of them are positive for mature neuronal marker (NF200), the establishment of

418   neural polarity is another aspect to confirm the transition to a mature neuronal

419   phenotype. Culturing of ONPs on aligned scaffolds and under neuralising

420   condition increased the expression of neuronal polarity markers (TAU and

421   MAP2) but the polarities of those positive cells were not yet to be specified.

422

423

424   **FIGURES**

425
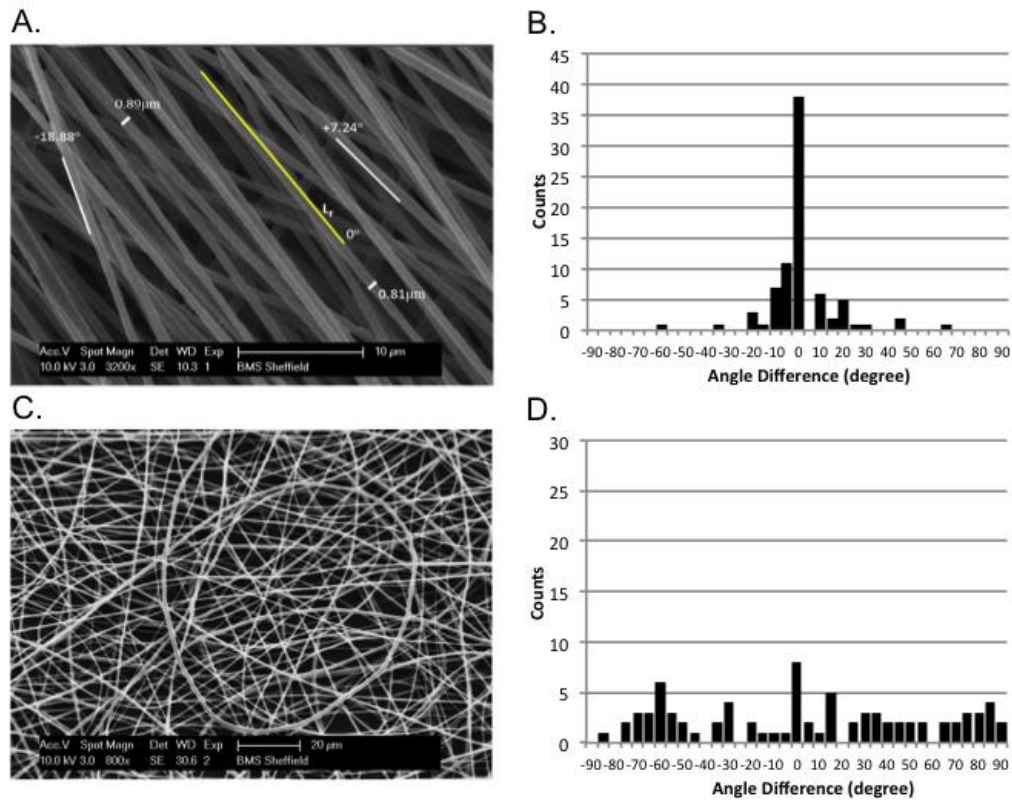
Figure 1. Electrospun fibres from optimized electrospinning parameters. (A) SEM image of PLLA aligned fibres and alignment analysis (scale bar = 10 μm). (B) Histogram of angle difference showing that most of the fibres are parallel to the reference line. (C) SEM image of random fibres collected with the lowest collector rotation speed (scale bar = 20 μm). (D) Histogram of angle difference on random fibres.
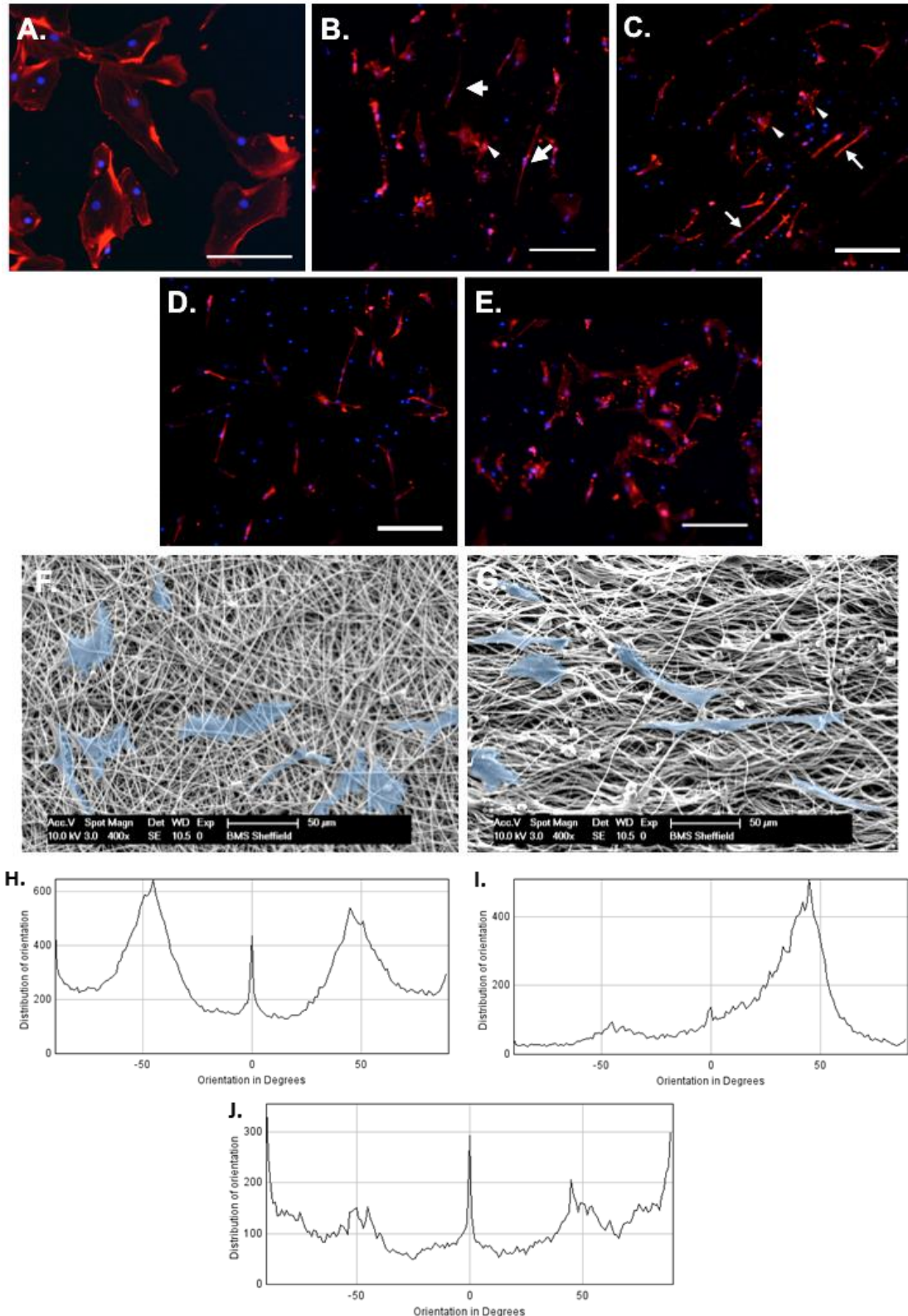
426
427
428
429
430
431

432

433

434

435

436

437

438

439

440

441

442

443

444

445

446

447

448

449

450

451

452 **Figure 2.** Actin staining showing ONP cell morphology on **(A)** tissue culture

453 plastic **(B)** PLLA aligned fibres after 3 days in culture **(C,D)** PLLA aligned

454 fibres after 14 days in culture **(E)** PLLA random fibres after 14 days in culture.

455 Scale bar=200μm. Scanning electron micrographs of the cells were shown on

456 **(F)** random and **(G)** aligned PLLA fibres. The cells were masked in blue for

457 the visibility. Scale bar=50μm. Distribution of cell orientation on tissue culture

458 plastic, PLLA aligned and random fibres were measured and shown as

459 histograms on (H), (I) and (J) respectively.
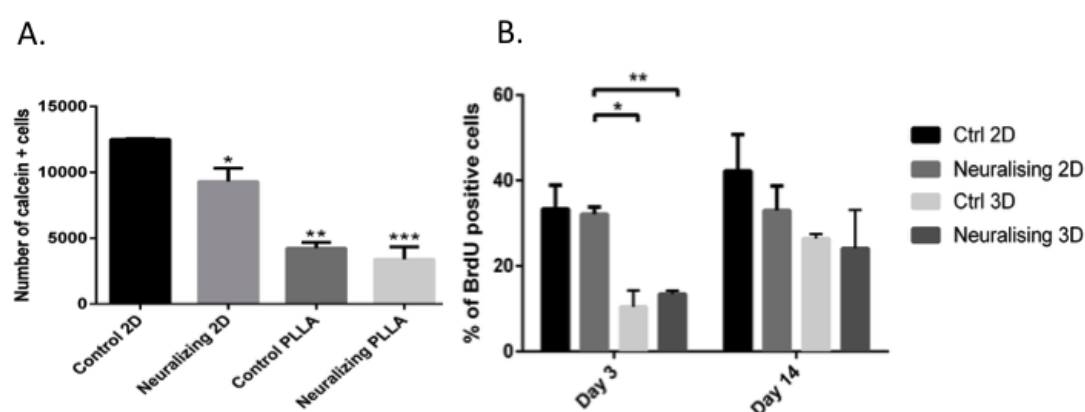
460

461 **Figure 3.** Viability and proliferation of ONPs on PLLA fibres. (A) Number of viable

462 ONPs on 1x1cm^2 PLLA aligned fibres after 14 days in culture. Data is mean±SD. (B)

463 ONPs proliferation after 3 and 14 days culture on PLLA aligned fibres. *p<0.05,
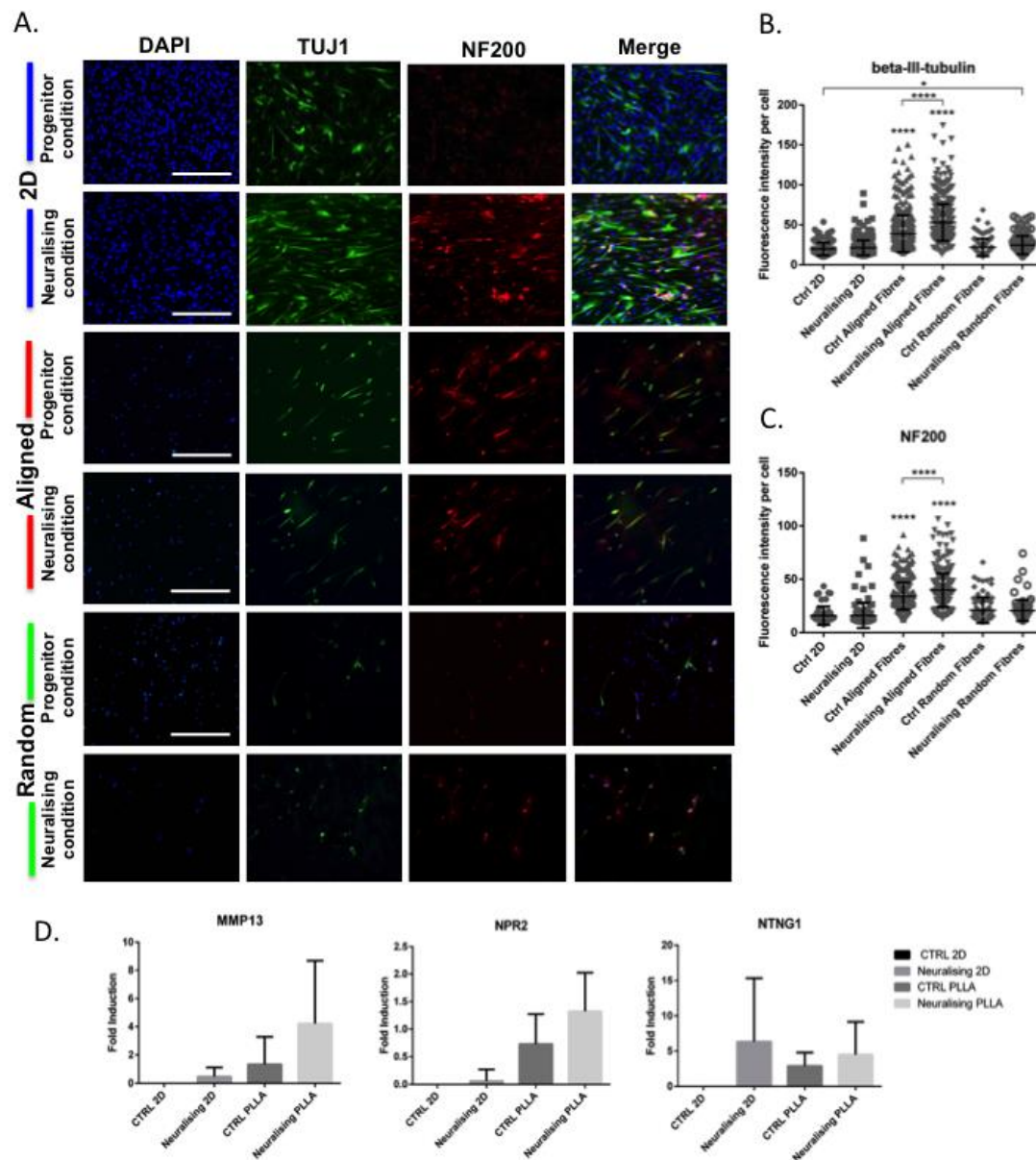
464 **p<0.01

465

466

Figure 4. The differentiation of ONPs on PLLA fibres. (A) Immunostaining of ONPs on 2D tissue culture plastic and 3D aligned PLLA fibres for neuronal markers, TUJ1 or ß-tubulinIII (green) and NF200 (red). Scale bar=400 µm. (B) Mean fluorescent intensity per cell of ß-tubulinIII and (C) NF200 on different culture materials. *p<0.05, ****p<0.0001 (D) The effect of aligned substrates on the expression of MMP13, NPR2 and NTNG1 in ONPs. Data is mean±SD.

473
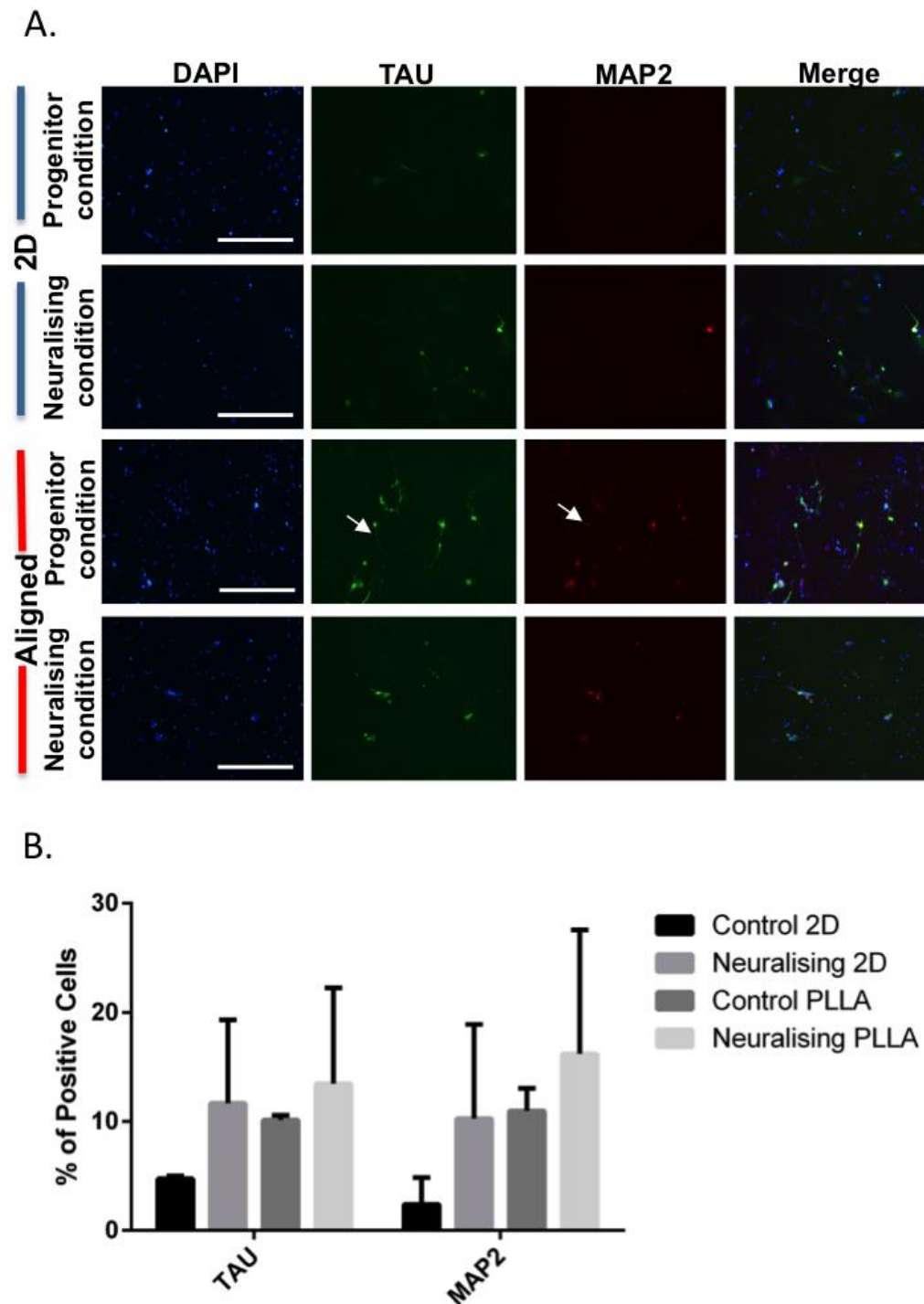
Figure 5. ONP polarization on PLLA aligned fibres. (A) Immunolabelling of neural polarity markers, TAU (green) and MAP2 (red) on ONPs. Scale bar=400 μm. (B) Percentage of TAU and MAP2 positive ONPs when cultured on different substrates for 14 days. Data shown are mean±SD.

CONCLUSIONS AND FUTURE WORKS

In summary, we have demonstrated that otic neural progenitors (ONPs) can attach, survive and be able to differentiate on aligned PLLA fibres. The physical cue (alignment of fibres) can help enhancing the differentiation of ONPs even in the absence of neuralising agents and guiding neurite extension along the alignment axis. In addition, it also influences changes on ONP morphology and the specification of neural polarity. This aligned PLLA scaffolds can also be further manipulated to facilitate the transplantation. A conduit could be made by rolling the PLLA electrospun sheet and seed it with ONPs and glial cells. These applications could be highly useful to develop new strategies to repair the auditory nerve.

ACKNOWLEDGEMENT

CONTRIBUTIONS

All authors participate in the designed and interpretation of the studies. KN performed the experiments, analysed the data and wrote the manuscript. MNR and GB contributed to the revision of the manuscript.

COMPETETING INTERESTS

The authors declare no conflict of interest.

REFERENCES

1. Groves, A. K., Zhang, K. D. & Fekete, D. M. The genetics of hair cell development and regeneration. *Annu. Rev. Neurosci.* **36,** 361–81 (2013).

2. Hu, Z. *et al.* Survival and neural differentiation of adult neural stem cells transplanted into the mature inner ear. *Exp. Cell Res.* **302,** 40–47 (2005).

3. Incesulu, A. & Nadol, J. Correlation of acoustic threshold measures and spiral ganglion cell survival in severe to profound sensorineural hearing loss: Implications for cochlear implantation. *Ann. Otol. Rhinol. Laryngol.* **107,** 906–911 (1998).

4. Chen, W. *et al.* Restoration of auditory evoked responses by human ES-cell-derived otic progenitors. *Nature* **490,** 278–282 (2012).

5. Lang, H., Schulte, B. A. & Schmiedt, R. A. Ouabain induces apoptotic cell death in type I spiral ganglion neurons, but not type II neurons. *JARO - J. Assoc. Res. Otolaryngol.* **6,** 63–74 (2005).

6. Burdick, J. A. & Mauck, R. L. *Biomaterials for Tissue Engineering Applications.* (Springer-Verlag Wien, 2011).

7. Discher, D. E., Mooney, D. J. & Zandstra, P. W. Growth factors, matrices, and

519   forces combine and control stem cells. *Science* **324,** 1673–7 (2009).

520   8.   Shibata, S. B. & Raphael, Y. Future approaches for inner ear protection and
521   repair. *Journal of Communication Disorders* **43,** 295–310 (2010).

522   9.   Clarke, J. C. *et al.* Micropatterned methacrylate polymers direct spiral ganglion
523   neurite and Schwann cell growth. *Hear. Res.* **278,** 96–105 (2011).

524   10.   Mattotti, M., Micholt, L., Braeken, D. & Kovačić, D. Characterization of spiral
525   ganglion neurons cultured on silicon micro-pillar substrates for new auditory
526   neuro-electronic interfaces. *J. Neural Eng.* **12,** 26001 (2015).

527   11.   Reich, U. *et al.* Differential fine-tuning of cochlear implant material-cell
528   interactions by femtosecond laser microstructuring. *J. Biomed. Mater. Res. -*
529   *Part B Appl. Biomater.* **87,** 146–153 (2008).

530   12.   Stöver, T. & Lenarz, T. [Biomaterials in cochlear implants].
531   *Laryngorhinootologie.* **88 Suppl 1,** S12–S31 (2009).

532   13.   Evans, A. R. *et al.* Laminin and fibronectin modulate inner ear spiral ganglion
533   neurite outgrowth in an in vitro alternate choice assay. *Dev. Neurobiol.* **67,**
534   1721–1730 (2007).

535   14.   Kikkawa, Y. S. *et al.* Growth factor-eluting cochlear implant electrode: impact
536   on residual auditory function, insertional trauma, and fibrosis. *J. Transl. Med.*
537   **12,** 280 (2014).

538   15.   Paasche, G. *et al.* Technical report: modification of a cochlear implant
539   electrode for drug delivery to the inner ear. *Otol. Neurotol.* **24,** 222–7 (2003).

540   16.   Pettingill, L. N., Richardson, R. T., Wise, A. K., O'Leary, S. J. & Shepherd, R.

541   K. Neurotrophic factors and neural prostheses: Potential clinical applications

542   based upon findings in the auditory system. *IEEE Transactions on Biomedical*

543   *Engineering* **54,** 1138–1148 (2007).

544   17.   Ryan, A. F., Wittig, J., Evans, A., Dazert, S. & Mullen, L. Environmental

545   micropatterning for the study of spiral ganglion neurite guidance. *Audiol.*

546   *Neurotol.* **11,** 134–143 (2005).

547   18.   Stover, T. *et al.* Development of a drug delivery device: using the femtosecond

548   laser to modify cochlear implant electrodes. *Cochlear Implant. Int* **8,** 38–52

549   (2007).

550   19.   Xie, J. *et al.* Neurotrophins differentially stimulate the growth of cochlear

551   neurites on collagen surfaces and in gels. *NEURAL Regen. Res.* **8,** (2013).

552   20.   Schwieger, J. *et al.* Neuronal survival, morphology and outgrowth of spiral

553   ganglion neurons using a defined growth factor combination. *PLoS One* **10,**

554   (2015).

555   21.   Santi, P. A. & Johnson, S. B. Decellularized ear tissues as scaffolds for stem

556   cell differentiation. *JARO - J. Assoc. Res. Otolaryngol.* **14,** 3–15 (2013).

557   22.   Chen, W. *et al.* Human fetal auditory stem cells can be expanded in vitro and

558   differentiate into functional auditory neurons and hair cell-like cells. *Stem Cells*

559   **27,** 1196–1204 (2009).

560   23.   Untergasser, A. RNAprep - Trizol combined with Columns. *Untergasser's Lab*

561   (2008).   at

562   <http://www.untergasser.de/lab/protocols/rna_prep_comb_trizol_v1_0.htm>

563   24.   Purves, D. *et al. Neuroscience.* (Sinauer Associate, Inc., 2008). doi:978-
564   0878937257

565   25.   Lu, C. C., Appler, J. M., Houseman, E. A. & Goodrich, L. V. Developmental
566   Profiling of Spiral Ganglion Neurons Reveals Insights into Auditory Circuit
567   Assembly. *J. Neurosci.* **31,** 10903–10918 (2011).

568   26.   NCBI. MMP13 matrix metallopeptidase 13 [Homo sapiens (human)]. (2016).
569   at <http://www.ncbi.nlm.nih.gov/gene/4322>

570   27.   Lu, C. C. *et al.* Mutation of Npr2 Leads to Blurred Tonotopic Organization of
571   Central Auditory Circuits in Mice. *PLoS Genet.* **10,** (2014).

572   28.   NCBI. NPR2 natriuretic peptide receptor 2 [Homo sapiens (human)]. (2016).
573   at <http://www.ncbi.nlm.nih.gov/gene/4882>

574   29.   NCBI. NTNG1 netrin G1 [Homo sapiens (human)]. (2016). at
575   <http://www.ncbi.nlm.nih.gov/gene/22854>

576   30.   Guillot, P. V, Cui, W., Fisk, N. M. & Polak, D. J. Stem cell differentiation and
577   expansion for clinical applications of tissue engineering. *J. Cell. Mol. Med.* **11,**
578   935–44 (2007).

579   31.   Schofield, R. The relationship between the spleen colony-forming cell and the
580   haemopoietic stem cell. *Blood Cells* **4,** 7–25 (1978).

581   32.   Li, L. & Xie, T. Stem cell niche: structure and function. *Annu. Rev. Cell Dev.*
582   *Biol.* **21,** 605–631 (2005).

583   33.   Liu, W., Thomopoulos, S. & Xia, Y. Electrospun nanofibers for regenerative

584   medicine. *Adv. Healthc. Mater.* **1,** 10–25 (2012).

585   34.   Xie, J., MacEwan, M. R., Schwartz, A. G. & Xia, Y. Electrospun nanofibers for
586   neural tissue engineering. *Nanoscale* **2,** 35–44 (2010).

587   35.   Schnell, E. *et al.* Guidance of glial cell migration and axonal growth on
588   electrospun nanofibers of poly-ε-caprolactone and a collagen/poly-[epsilon]-
589   caprolactone blend. *Biomaterials* **28,** 3012–3025 (2007).

590   36.   Shen, Y. *et al.* Guidance of olfactory ensheathing cell growth and migration on
591   electrospun silk fibroin scaffolds. *Cell Transplant.* **19,** 147–157 (2010).

592   37.   Xie, J. *et al.* The differentiation of embryonic stem cells seeded on electrospun
593   nanofibers into neural lineages. *Biomaterials* **30,** 354–362 (2009).

594   38.   Hurtado, A. *et al.* Robust CNS regeneration after complete spinal cord
595   transection using aligned poly-l-lactic acid microfibers. *Biomaterials* **32,** 6068–
596   6079 (2011).

597   39.   Kim, Y. tae, Haftel, V. K., Kumar, S. & Bellamkonda, R. V. The role of aligned
598   polymer fiber-based constructs in the bridging of long peripheral nerve gaps.
599   *Biomaterials* **29,** 3117–3127 (2008).

600   40.   Bhardwaj, N. & Kundu, S. C. Electrospinning: A fascinating fiber fabrication
601   technique. *Biotechnology Advances* **28,** 325–347 (2010).

602   41.   Binder, C., Milleret, V., Hall, H., Eberli, D. & Lühmann, T. Influence of micro
603   and submicro poly(lactic-glycolic acid) fibers on sensory neural cell locomotion
604   and neurite growth. *J. Biomed. Mater. Res. - Part B Appl. Biomater.* **101,**
605   1200–1208 (2013).

606   42.   Christopherson, G. T., Song, H. & Mao, H. Q. The influence of fiber diameter

607   of electrospun substrates on neural stem cell differentiation and proliferation.

608   *Biomaterials* **30,** 556–564 (2009).

609   43.   Baker, B. M. & Chen, C. S. Deconstructing the third dimension - how 3D

610   culture microenvironments alter cellular cues. *J. Cell Sci.* **125,** 3015–3024

611   (2012).

612   44.   Gerardo-Nava, J. *et al.* Human neural cell interactions with orientated

613   electrospun nanofibers in vitro. *Nanomedicine (Lond).* **4,** 11–30 (2009).

614   45.   Lim, S. H., Liu, X. Y., Song, H., Yarema, K. J. & Mao, H. Q. The effect of

615   nanofiber-guided cell alignment on the preferential differentiation of neural

616   stem cells. *Biomaterials* **31,** 9031–9039 (2010).

617   46.   Liu, X. *et al.* Guidance of neurite outgrowth on aligned electrospun polypyrrole/

618   poly(styrene-beta-isobutylene-beta-styrene) fiber platforms. *J. Biomed. Mater.*

619   *Res. - Part A* **94,** 1004–1011 (2010).

620   47.   Arimura, N. & Kaibuchi, K. Neuronal polarity: from extracellular signals to

621   intracellular mechanisms. *Nat. Rev. Neurosci.* **8,** 194–205 (2007).

622   48.   Adler, C. E., Fetter, R. D. & Bargmann, C. I. UNC-6/Netrin induces neuronal

623   asymmetry and defines the site of axon formation. *Nat. Neurosci.* **9,** 511–518

624   (2006).

625   49.   Whitford, K. L., Dijkhuizen, P., Polleux, F. & Ghosh, A. Molecular control of

626   cortical dendrite development. *Annu. Rev. Neurosci.* **25,** 127–49 (2002).

627   50.   Da Silva, J. S., Hasegawa, T., Miyagi, T., Dotti, C. G. & Abad-Rodriguez, J.

628   Asymmetric membrane ganglioside sialidase activity specifies axonal fate. *Nat*

629   *Neurosci* **8,** 606–615 (2005).

630   51.   Huang, E. J. & Reichardt, L. F. Trk Receptors: Roles in Neuronal Signal

631   Transduction. *Annu. Rev. Biochem.* **72,** 609–642 (2003).

632